Structural, electrical and optical properties of sol–gel derived yttrium doped ZnO films

Ravinder Kaur, A. V. Singh, and **R. M. Mehra**[*]

Department of Electronic Science, University of Delhi South Campus, New Delhi – 110021, India

Undoped and yttrium doped zinc oxide thin films have been deposited on corning glass by dip coating technique. The effect of doping (0–4 wt%) and annealing temperature (300–500 °C) on the structural, optical and electrical properties of the produced films have been investigated. All the films show polycrystalline nature at an annealing temperature of 350 °C. The preferential *c*-axis growth with lowest full width at half maximum of (002) reflection peak is seen only up to an optimum annealing temperature. A blue shift in the absorption edge is observed both, with increase in dopant concentration and annealing temperature. The electrical resistivity of the films decreases by doping with yttrium. The lowest resistivity of 3.5×10^{-2} Ω cm and an average transmittance of 86% in the visible range has been obtained in YZO films doped with 3 wt% of yttrium and annealed at 450 °C.

1 Introduction

The increased demand for transparent conducting thin films for optoelectronic devices [1], liquid crystal displays, heat mirrors and multilayer photothermal conversion system [2] has promoted interest in electro optical properties of zinc oxide (ZnO) thin films. These films have the advantage of high mechanical stability, non-toxic nature, large electronic band gap [3] of 3.3 eV and conductivities that can be controlled by either selecting the nonstoichiometry and/or appropriate dopants. The nonstoichiometric ZnO films although have excellent electrical and optical properties, but they are not chemically stable at high temperatures and this makes them unusable for practical applications [4]. However, doped films can be made to have very stable electrical and optical properties [5]. The doping effect of In, Al and Ga in ZnO has been frequently reported by many research groups [4, 5] but the doping effect of a rare-earth impurity such as Sc, Y has been scarcely reported, although their ion radius is very close to that of zinc making them compatible for doping. The effect of Y doping in ZnO films, prepared by spray pyrolysis technique, on luminescence properties has been reported by M. O. Abou-Helal et al. [6]. Y. Shimizu et al. [7] have shown that the sensitivity of hydrogen sensors derived by YZO is anticipated to be related to decrease in grain size by Y doping. T. Minami et al. [8] have reported the detailed investigation of the electrical and optical properties of Sc doped ZnO films prepared by d.c. magnetron sputtering technique. However, sol-gel is a low cost, non-vacuum and low substrate temperature deposition technique as compared to the other techniques. Since zinc belongs to the group of elements, which form polymeric hydroxides, a fundamental requirement for sol-gel chemistry, this technique can be easily used to deposit thin films of zinc oxide [5, 9].

[*] Corresponding author: e-mail: rammehra2003@yahoo.com, Phone: +91 11 24105849; Fax: +91 11 26876876

This paper describes the preparation and characterization of the yttrium doped zinc oxide (YZO) films by sol-gel technique using ethanol as a solvent and diethanolamine (DEA) as a sol-gel stabilizer. It is shown in our earlier work [10] that DEA acts as the most efficient stabilizer to obtain good quality films. Effect of Y doping on structural (preferred orientation, surface morphology), electrical (resistivity, carrier concentration and Hall mobility) and optical properties (transmittance, band gap) is reported. The effects of annealing temperature on the above said properties of ZnO thin films were investigated in the temperature range 300–500 °C.

2 Experiment

A precursor solution of ZnO, about 0.2 M in concentration was prepared from zinc acetate $(Zn(CH_3CO_2)_2 \cdot 2H_2O$, purity 99.5%) dissolved in anhydrous ethanol. It was observed that the solutions prepared with a concentration greater than 0.2 M did not remain stable for a long time. Yttrium nitrate hexahydrate $(Y_2NO_3 \cdot 6H_2O)$ was used as the dopant (1–4 wt%) in the present study. The mixture so obtained was stirred in a magnetic stirrer for about 4 hrs at room temperature, but it remained milky. An equimolar amount of DEA was added to the solution drop wise to eliminate the obtained turbidity and the precipitates completely. The resultant solution was very clear, transparent and homogenous and was used after 48 hrs for film deposition.

Glass substrates, after being cleaned with acetone and methanol in an ultrasonic bath for 20 minutes each, were dipped in the solution and dried at 300 °C for 20 minutes. This cycle was repeated 10–15 times. The thickness of the films was in the range of 200–250 nm. The deposited films were annealed in air in the temperature range of 300–500 °C for 1 hr.

The structural properties of the films were investigated by Phillips–Holland X-ray diffractometer (Model PW 1830/00). The thickness of the films was measured by the DEKTECK[3-ST] surface profilometer. The electrical resistivity and Hall coefficient of the films at room temperature was measured by van-der Pauw technique. The optical transmittance measurements were carried out in the wavelength range of 200–800 nm using a double beam SHIMADZU-330 spectrophotometer. The composition wt% of Yttrium to zinc, of YZO films was found to be nearly equal to that in the solution as determined by the Elemental Dispersion Analysis using X-rays (EDAX) measurements.

3 Results and discussion

3.1 Structural properties

As grown YZO (0–4 wt% Y) films show an amorphous nature whereas, films annealed in the temperature range of 350–500 °C exhibit an evidence of conversion from the amorphous to polycrystalline structure with (100), (002) and (101) X-ray diffraction peaks. As the annealing temperature is increased from 350 °C to 450 °C, the (002) reflection peak becomes intense and sharper as compared to the other peaks, indicating a tendency in the *c*-axis preferential growth of the films. Figure 1 shows the variation of full
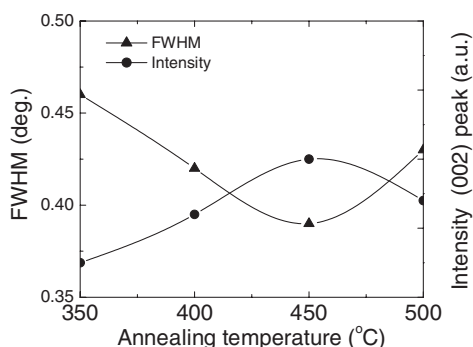

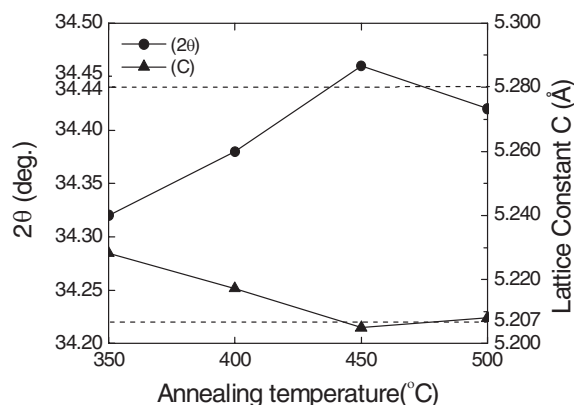**Fig. 1** Effect of annealing temperature on FWHM and intensity of (002) peak of YZO films (3 wt%).

Fig. 2 Effect of annealing temperature on lattice constant '*c*' and diffraction angle '2θ' of (002) peak of YZO films (3 wt%).
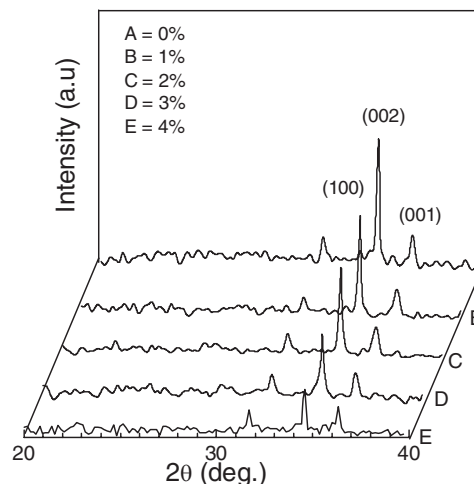
Fig. 3 XRD patterns of YZO films of different Y concentrations annealed at 450 °C in air.

width at half maximum (FWHM) and intensity of (002) peak with annealing temperature for YZO (3 wt%) films. It is observed that the peak intensity increases and FWHM decreases with increase in annealing temperature till 450 °C. Since the value of FWHM is inversely proportional to the grain size, it implies that the grain size improves with the increase in annealing temperature [11] along with an improvement in crystallinity. However, a further increase in annealing temperature results in a decrease in intensity and an increase in FWHM which indicate a decrease in *c*-axis orientation and the grain size. This may be due to the contamination of alkali ions from the glass substrate [12].

Figure 2 shows the variation of '2θ' (diffraction angle) of (002) peak and lattice constant '*c*' with the annealing temperature. A shift in the (002) peak position to a slightly higher 2θ value is observed with the increase in the annealing temperature and it approaches the powder value of 34.44° at a temperature of 450 °C. Correspondingly the value of *c* decreases with an increase in annealing temperature. This indicates a reduction in the tensile stress with annealing [13], which may be due to the large coefficient of linear expansion of YZO films in comparison with the glass substrate with increase in the annealing temperature. However, with further increase in the temperature, *c* increases slightly. The larger value of *c* at 350 °C shows that the unit cell is elongated along *c*-axis, and compressive forces act in the plane of the films. These compressive forces become weaker as the annealing temperature exceeds 350 °C, resulting in the decrease in *c* value. Thus with the increase in annealing temperature, shrinkage of *c* along with the improvement in *c*-axis orientation is seen. Matsuoka et al. [14] have also observed shrinkage of lattice constant in Al doped ZnO films due to the increase of substrate temperature.

Figure 3 shows the X-ray diffraction patterns of the YZO films annealed at optimized temperature (450 °C) for different dopant concentrations. It is observed that for Y greater than 3 wt% the intensity of (002) peak decreases sharply with a subsequent increase in FWHM, implying the degradation in the crystallinity and reduction in grain size of the film.

3.2 Electrical properties

The sign of Hall coefficient shows that all the YZO films are n-type in nature. Resistivity (ρ), carrier concentration (n) and Hall mobility (μ_{H}) as functions of Y content in the films are shown in Fig. 4. It is seen from the figure that ρ decreases sharply as the Y concentration is increased up to 3 wt%. Correspondingly n is found to increase while there is a gradual reduction in μ_{H}. The substantial increase in n confirms that Y acts as an effective donor in ZnO films.
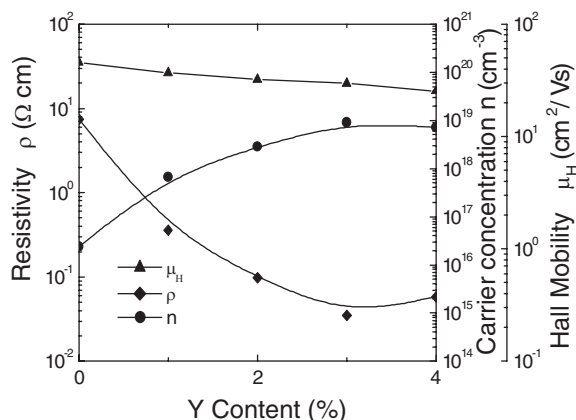
Fig. 4 Resistivity (ρ), carrier concentration (n) and Hall mobility (μ_H) as a function of Y wt% annealed at 450 °C in air.

The above behavior of n suggests that the increased carrier concentration is due to the contribution from doping ion Y^{3+} on substitution site of Zn^{2+} ions and/or from interstitial zinc atoms. As the doping level is increased, more dopants occupy lattice sites of zinc atom, which results in an enhanced number of charge carriers. However, after a critical doping i.e. 3 wt% of Y in our case, the carrier concentration tends to saturate and resistivity starts increasing. This is probably because of the limited solubility of yttrium in ZnO. W. Tang et al. [5] have shown a similar effect in ZnO: Al films. The decrease in mobility at higher doping may be due to scattering from grain boundaries and defects produced by doping, which is also supported by the XRD analysis [15].

The variation of ρ, n and μ_H of YZO films as a function of annealing temperature are shown in Fig. 5. The mobility is found to increase with the annealing temperature up to 450 °C, which is due to the improvement of crystalline structure of the films as observed by XRD analysis (Fig. 1). The value of μ_H is found in the range of 35 to 16.1 cm²/Vs. Several workers have also reported μ_H in the same range in the case of Al doped ZnO [5, 16, 17]. It is also observed that n increases with the increase in annealing temperature. It was observed that at an optimized annealing temperature the grain size and crystallinity attain the maximum value. This increase in grain size means a decrease in grain boundaries and pores in the annealed films as compared to the as deposited films. So the number of electron trap states reduces and hence the carrier concentration increases.

The slight increase in resistivity of the films at temperature above 450 °C may be due to the structural degradation. The lowest resistivity of 3.5×10^{-2} Ω cm is obtained in YZO films doped with 3 wt% of Y and annealed at 450 °C.
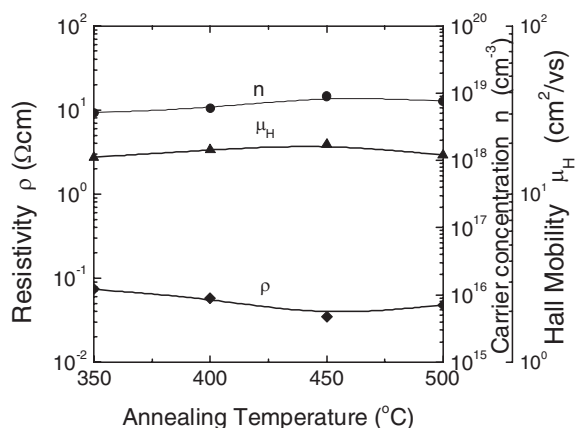

Fig. 5 Resistivity (ρ), carrier concentration (n) and Hall mobility (μ_H) as a function of annealing temperature for 3 wt% Y.
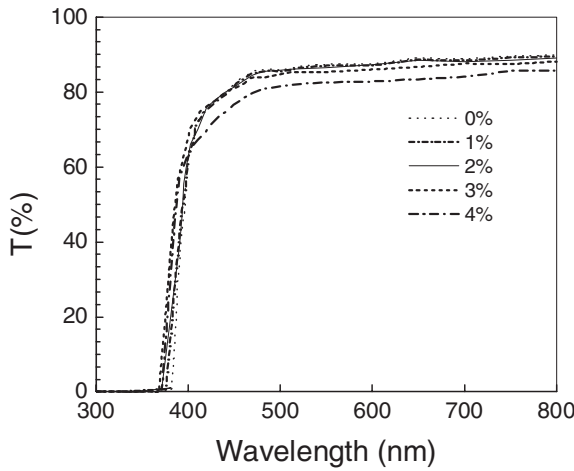
Fig. 6 Variation of transmittance (*T*) as a function of Y concentration in the wavelength range 200–800 nm for YZO films annealed at 450 °C.

3.3 Optical properties

As shown in Fig. 6 the average transmittance *T*, of the films having Y (0–3 wt%) in the visible region is higher than 85%. At 4 wt% of Y, the transmittance decreases to 82.8%, which may be due to the increase in the defects produced in YZO films at higher dopant concentration or due to the increase in the absorption coefficient.

The optical band gap 'E_g' was calculated using the Tauc's plot as shown in Fig. 7.

An increase in E_g is observed with Y doping up to 3 wt%. However, with further increase in Y doping the value of E_g decreases. The dependence of E_g on carrier concentration is analyzed considering the Burstein Moss model [18] for the absorption edge shift ΔE^{BM} in an n-type semiconductor which is given by

$$\Delta E^{BM} = \left(3\pi^2 N\right)^{2/3} \frac{\hbar^2}{2m_{vc}^*},$$ (1)

where m_{vc}^* is a reduced effective mass and is given by

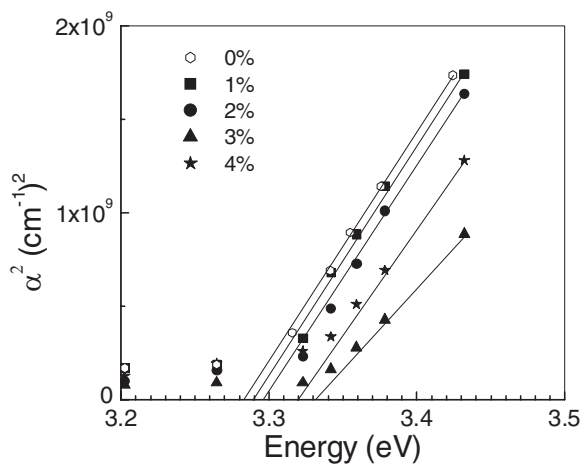$$\frac{1}{m_{vc}^*} = \frac{1}{m_c^*} + \frac{1}{m_v^*}$$ (2)

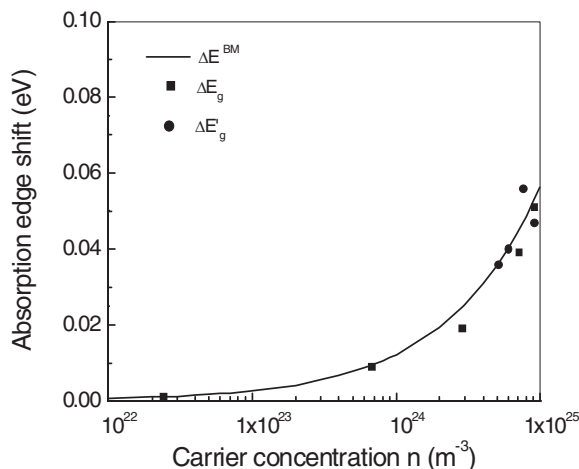**Fig. 7** Band gap calculation for YZO films using Tauc's plot.

Fig. 8 Absoption edge shift as a function of carrier concentration. Solid line shows the calculated ΔE^{BM}, (■) shows ΔE_g (experimental) due to variation in dopant concentration and (●) shows $\Delta E'_g$ (experimental) for different annealing temperatures.

where m_c^* is the effective mass in the conduction band and m_v^* is the effective mass in the valance band. The values of the effective masses have been taken from our earlier work [16]. The change ΔE_g in E_g due to variation in dopant concentration and ΔE^{BM} with n is shown in Fig. 8.

The transmittance and the optical band gap of YZO films with 3 wt% of Y for different annealing temperatures are given in Fig. 9. It is observed that T increases with increase in annealing temperature up to 450 °C. But with further increase in temperature it decreases. The initial increase in T is due to the improvement in the crystallinity and microstructure with an increase in annealing temperature (Fig. 1). The observed decrease in T with further increase in annealing temperature is due to the degradation of crystallinity of YZO films as supported by our XRD analysis. A change $\Delta E'_g$ in E_g is also observed with annealing. The variation of $\Delta E'_g$ and ΔE^{BM} with n as a function of annealing temperature is also shown in Fig. 8. It is clear from the figure that the Burstein–Moss model satisfactorily takes into account the change in band gap both, due to the variation in dopant concentration and the annealing temperature.

4 Conclusions

Yttrium doped n-type ZnO films have been obtained by sol-gel process. The preferential *c*-axis growth, the lowest resistivity and the highest transmittance is observed for 3 wt% of Y at an optimized annealing temperature of 450 °C. The shift in band gap with yttrium concentration as well as with annealing temperature has been attributed to the change in carrier concentration, in accordance with the Burstein–Moss model. Yttrium doping in ZnO has also yielded the value of mobility similar to what is reported in
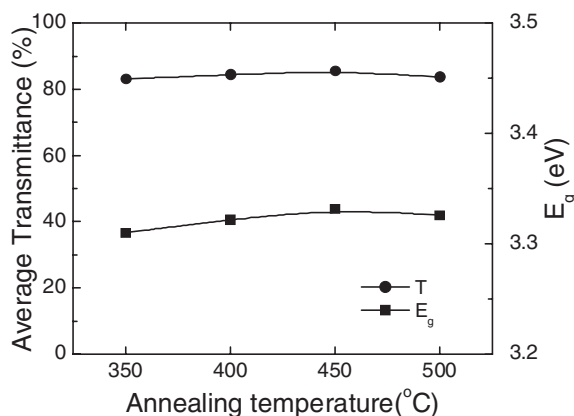

Fig. 9 Transmittance and band gap as a function of annealing temperature for 3 wt% YZO films.

phys. stat. sol. (a) **202**, No. 6 (2005) / www.pss-a.com

1059

the case of Al doping. Further investigations are on the way to develop YZO films having higher carrier concentration in order to be used as transparent conducting electrode in solar cells.

References

[1] D. C. Look, D. C. Reynolds, J. R. Sizelove, R. L. Jones, C. W. Litton, G. Cantwell, and W. C. Harsch, Solid State Commun. **105**, 399 (1998).
[2] K. L. Chopra, S. Major, and D. K. Pandya, Thin Solid Films **102**, 1 (1983).
[3] A. Malik, A. Seco, P. Nunes, and M. Vieira, MRS Displays Technologies, Vol. 471 (San Francisco, USA, 2–8 April 1997).
[4] J. F. Chang, W. C. Lin, and M. H. Hon, Appl. Surf. Sci. **183**, 18 (2001).
[5] W. Tang and D. C. Cameron, Thin Solid Films **238**, 83 (1994).
[6] M. O. Abou-Helal and W. T. Seebar, J. Non-Cryst. Solids **218**, 139 (1997).
[7] Y. Shimizu, F. Lin, Y. Takao, and M. Egashira, J. Am. Ceram. Soc. **81**, 1633 (1998).
[8] T. Minami, T. Yamamoto, and T. Miyata, Thin Solid Films **366**, 63 (2000).
[9] Y. Kokubun, H. Kimoro, and S. Nagakomi, Jpn. J. Appl. Phys. **42**, L904 (2003).
[10] R. Kaur, A. V. Singh, and R. M. Mehra, Mater. Sci. **22**, 3 (2004).
[11] T. Minami, H. Sato, S. Takata, N. Ogawa, and T. Mouri, Jpn. J. Appl. Phys. **31**, L1106 (1992).
[12] J. R. Bosnell and R. Waghorne, Thin Solid Films **15**, 141 (1973).
[13] S. Takada, J. Appl. Sci. **73**, 4739 (1993).
[14] M. Matsuoka, Y. Hoshi, and M. Naoe, J. Appl. Phys. **63**, 2098 (1998).
[15] T. Minami, H. Nanto, and S. Takata, Jpn. J. Appl. Phys. **71**, 880 (1992).
[16] A. V. Singh, R. M. Mehra, A. Yoshida, and A. Wakahara, J. Appl. Phys. **95**, 3640 (2004).
[17] H. Kim, C. M. Gilmore, J. S. Horwitz, A. Pique, H. Murata, G. P. Kushto, R. Schlaf, Z. H. Kafafi, and D. B. Chrisey, Appl. Phys. Lett. **76**, 259 (2000).
[18] E. Burstein, Phys. Rev. **93**, 632 (1954).